

Characteristics of the synchronization of brain activity imposed by finite conduction velocities of axons

International Journal of Bifurcation and Chaos 10: 2307-2322, 2000.

Walter J Freeman

Division of Neurobiology LSA 129
Department of Molecular & Cell Biology
University of California
Berkeley CA 94720-3200

Tel 510-642-4220 Fax 510-643-6791
e-mail: wfreeman@socrates.berkeley.edu

Running title:

Synchronization of Brain Activity

Key words:

brain dynamics, chaos, EEG, oscillations, phase gradients, synchronization

Abstract

The electrical activity of neurons in brains fluctuates erratically both in terms of pulse trains of single neurons and the dendritic currents of populations of neurons. Obviously the neurons interact with one another in the production of intelligent behavior, so it is reasonable to expect to find evidence for varying degrees of synchronization of their pulse trains and dendritic currents in relation to behavior. However, synaptic communication between neurons depends on propagation of action potentials between neurons, often with appreciable distances between them, and the transmission delays are not compatible with synchronization in any simple way. Evidence is on hand showing that the principal form of synchrony is by establishment of a low degree of covariance among very large numbers of otherwise autonomous neurons, which allows for rapid state transitions of neural populations between successive chaotic basins of attraction along itinerant trajectories. The small fraction of covariant activity is extracted by spatial integration upon axonal transmission over divergent-convergent pathways, through which a remarkable improvement in signal:noise ratio is achieved. The raw traces of local activity show little evidence for synchrony, other than zero-lag correlation, which appears to be largely a statistical artifact. Brains rely less on tight phase-locking of small numbers of repetitively firing neurons and more on low degrees of cooperativity achieved by order parameters influencing very large numbers of neurons. Brains appear to be indifferent to and undisturbed by widely varying time and phase relations between individual neurons and even large semi-autonomous areas of cortex comprising their cooperative neural masses.

Acknowledgments

This work was supported by a grant MH06686 from the National Institute of Mental Health, by a grant N00014-90-J-4054 from the Office of Naval Research and by a grant from the ARO MURI DAAH04-96-1-0341. I am deeply grateful for the dedicated assistance of John M. Barrie and Brian C. Burke in acquisition of data, programming, analysis and illustration of the data, and to Robert Kozma for discussion of the theory.

1. Introduction

Brain activity is observed at three main space-time scales. At the microscopic scale are the pulses (action potentials) of single neurons measured in milliseconds and microns. At the macroscopic scale are the domains of high metabolic demand that are imaged in seconds and centimeters (cm) by a variety of techniques for measuring the spatial patterns of cerebral blood flow. In between at the mesoscopic scale of millimeters (mm) and tenths of a second are the patterns of the massed dendritic potentials seen in electroencephalographic (EEG) recordings from waking and sleeping brains. These waves have oscillations in several low frequency ranges, such as theta (3-7 Hz), alpha (8-12 Hz), beta (13-30 Hz), and gamma (30-100 Hz). Long stretches of recordings give broad spectra roughly conforming to " $1/f^2$ ", which have suggested to many researchers the possibility that this activity is governed by chaotic attractors instead of limit cycles embedded in noise. This interesting hypothesis has been pursued with the aid of models derived from deterministic chaotic systems, such as twist-flip maps, Lorenz, Rössler and Chua attractors. These low-dimensional models have engendered highly successful algorithms such as those of Takens, Grassberger, Procaccia and Guckenheimer for estimating the correlation dimensions and Lyapunov exponents of these models. This success has led to efforts to model the cognitive functions of sensory cortices in the realm of pattern classification with networks of chaotic elements that are coupled by nearest neighbor or next to nearest neighbor with weighted connections. The proper response of such systems would be synchronization or phase locking of an array of chaotic elements into one of a set of global chaotic attractors, after suitable training to form the attractor landscape.

Attempts to develop and apply such models by calculating correlation dimensions and related measures from EEGs have not succeeded in converging to reliable numbers (Rapp, 1993; Freeman and Jakubith, 1993). The failure is partly due to an assumption that the stationarity and autonomy of the models holds also for brain systems, which is inappropriate because brains are continuously engaged with their bodies and environments, and they undergo repeated state transitions in multiple time scales. Most importantly, the methods fail because the EEG traces recorded from brains are heavily invested with various kinds of noise, for some of which the dimensions are infinite. Estimates of correlation dimension invariably increase with the duration of the sample.

The aims of this report are to sketch the mechanism by which EEG waves are generated, to estimate the degree of synchrony among the participating neurons that is required to form the waves, and to describe the spatial patterns of phase that are revealed by multichannel recordings of the waves. The conclusion is offered that the EEG manifests a small fraction of the total variance of the neurons in the generating populations that is covariant (synchronous), and that the spatial pattern of phase reveals a critical determinant of the size of the areas of self-organized activity in sensory cortices (~ 1 cm), namely the group velocity of the state transitions by which spatiotemporal patterns of cortical activity emerge, thereafter being successfully extracted from noise by the targets of cortical transmissions.

2. Origins of steady state background activity

The cerebral cortex of vertebrates grows a type of cell that is unique to nervous systems, because each cell extends long branching filaments into its surround and makes synaptic connections with thousands of others (Figure 1). The input threads are dendrites, and each neuron may have up to 4 or 5 dendritic branches. The output thread is an axon, and while each neuron has only one, it typically has many branches that multiply its signal.

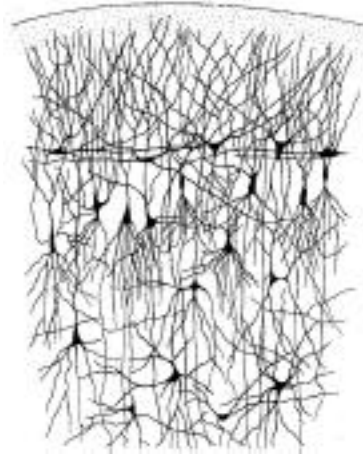


Figure 1. An example is shown of the Golgi technique for impregnating neurons with silver to display their cell bodies and their branching filaments (axons and dendrites) making functional connections (synapses) with each other. These cortical cells are grouped in layers stacked parallel under the surface. The Golgi technique, when it is successful, displays < 1% of the neurons, giving the illusion of a sparse network, when in fact the tissue is exceedingly dense, each neuron making connections with many thousands of other neurons. Redrawn from Ramón y Cajal (1911).

The growth begins early in gestation, accelerates during infancy and childhood, and continue throughout adult life. This process of growth may be comparable to the property of a sparsely connected random graph, in which the connection density among nodes is gradually increased. Above a certain "percolation threshold" a "giant component" forms that incorporates lesser components (Bollabás 1985). The axons generate pulses; the dendrites generate graded waves of current. Each synapse acts like a small battery that is turned on by a pulse, and that drives current inwardly at excitatory synapses and outwardly at inhibitory synapses (Figure 2).

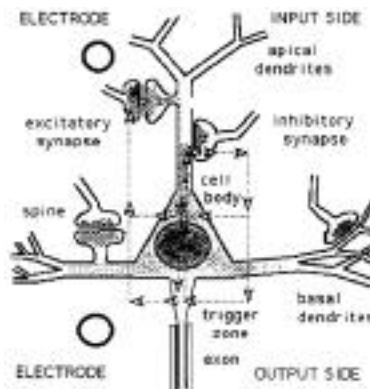


Figure 2. A schematic diagram of a neuron is used to show how a pulse arriving at a synapse triggers the flow of loop current, inwardly at excitatory synapses, outwardly at inhibitory synapses, and across the membrane everywhere. Thousands of loop currents sum at the trigger zone and determine the probability of firing. The same current sum crosses the extracellular space where it sums with the currents of other neurons in the neighborhood, thereby giving access to the mesoscopic local mean field through the EEG. From Freeman 1992.

The intracellular limb of the loop currents converge to the base of the dendritic trees and cross the cell membrane in the opposite direction at the base of the axonal tree, where at the trigger zone the sum of the currents determines the probability of firing at each instant and the relative frequency over stated time periods, net outward current increasing the probability and net inward current decreasing it. The function of the single neuron is to provide the surface area for thousands of synapses, the dendritic channels to converge and integrate the currents, the trigger zone to convert the sum of current to a pulse train, and the axon tree to multiply and distribute the output without attenuation with distance, but at the cost of conduction delay. Neurons grow to adapt to the distance of transmission by their size. Small neurons transmit over short distances < 1 mm at velocities < 2 m/s. Large neurons transmit over long distances (cm to meters) at velocities of 10-100 m/s. Pulse trains are re-converted to waves at synapses and smoothed by passive membranes acting as first order low-pass filters having time constants of 5-10 ms.

The neurons in the outer shell of the forebrain are organized into layers with neurons having their receiving dendrites oriented both perpendicular (apical dendrites) and parallel (basal dendrites) to the surface. Their axons end in synapses mostly within the layers formed by the cell bodies. The larger neurons that send their axons out of the cortex give off side branches that return into the area in which the transmitting neurons are located. Most of these recurrent synaptic connections are between excitatory neurons; they excite each other. Early in embryonic life the density of connections is low, and firing of pulses is sporadic as determined by individual neurons. As cortex matures the threads continue to extend, branch, and form new synapses (Freeman 1999). At some point the connection density surpasses a threshold of unity feedback gain, meaning each neuron receives more pulses than it gives. At this point a collection of neurons becomes an interactive population with self-sustaining activity that is limited by the refractory period following each pulse, when the neuron is recovering and briefly cannot fire.

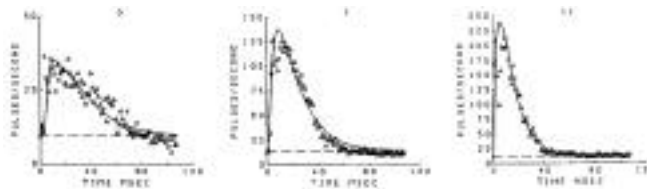


Figure 3. Neurons form populations by synaptic interactions. Mutual excitation gives a sustained level of background firing indicated by the dashed lines. This activity is governed by a point attractor. Its stability is shown by the impulse responses to electrical stimulation of the population. The increase in firing density is proportional to stimulus intensity, and so also is the decay rate from the peak. The decay rate extrapolates to zero at threshold (zero response amplitude), revealing the existence of a zero eigenvalue (a stable pole at the origin of the complex plane) specifying unity gain in a positive feedback loop. From Freeman 1974.

Whereas the collection of neurons (a noninteractive KO set - Freeman 1975) is governed by a zero level point attractor, the excitatory population (a KI_e set) is governed by a non-zero (positive) point attractor. The activity of such an excitatory population has the form of steady state pulse trains, each of which statistically resembles a Poisson process with a dead time, and for which the autocorrelation and cross correlations with other trains rapidly go to zero. The feedback pathway for each neuron to itself through innumerable synaptic chains can be modeled as a one-dimensional diffusion process (Freeman 1975), so the impulse response is a gamma distribution of order one-half, and the return to each neuron

is randomized. Each area of cortex containing millions of interconnected neurons generates a field of nearly white noise, up to the frequency limit imposed by the durations of the pulses (~ 1 ms). The dendritic currents generate EEGs by flowing across the tissue resistance, revealing slow irregular fluctuations (< 1 Hz) about a non-zero mean value.

When the KI_e population is driven by an excitatory electrical stimulus constituting a Dirac delta function, the impulse response of the excitatory population (Figure 3) shows a sudden increase in firing probability followed by an exponential decay to the background level. The decay rate is proportional to the stimulus intensity and response amplitude. As the response amplitude is decreased toward zero, the decay rate approaches zero, which reflects the stability property of the point attractor that regulates the activity level and the set point of the population. The neurons operating at the microscopic level generate noise, whereas the population generates a mesoscopic order parameter that determines the mean firing density, which constitutes an excitatory drive or bias for the same population and for other populations that receive the sustained activity.

3. Origins of aperiodic oscillations

At a stage of development before or shortly after birth, inhibitory interneurons appear, which form a KI_i set, and which support negative feedback by interacting with a KI_e set in forming a KII set. The impulse response becomes oscillatory, revealing the characteristic frequency of the KII population (Figure 4) both in the form of evoked potential in the wave

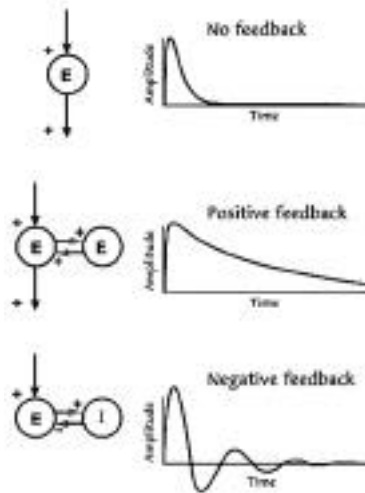


Figure 4. The open loop response (top trace) of a KO population conforms to the classic postsynaptic potential of single neurons. Positive feedback (mutual excitation and mutual inhibition) defining KI sets gives monotonic impulse responses (see Figure 3). Negative feedback in KII sets is sustained by interactions between excitatory and inhibitory KI sets. Both types of feedback can be stable or unstable. From Freeman 1975.

mode and the post stimulus time histogram in the pulse mode (Freeman 1975). The relations between the pulses and waves in the sustained background activity are visualized in a 2-D table by computing the probability of pulse firing conditional on EEG amplitude and time lag. The distribution of EEG amplitudes characteristically is nearly Gaussian, and the interval histograms of the pulse trains of single neurons decay exponentially with time in conform to a Poisson distribution, but with a short-lasting refractory period after each pulse (Figure 5).

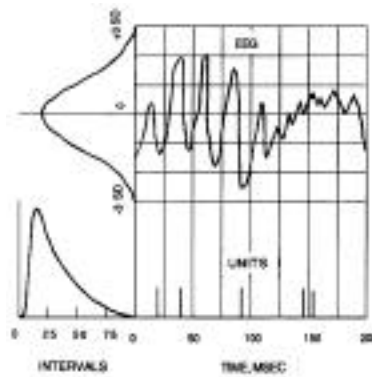


Figure 5. The raw data are shown for calculating the relation between microscopic pulses typically having an interval histogram like that of a Poisson process with a dead time (the refractory periods) and the mesoscopic EEG (extracellular dendritic potentials) that have a nearly Gaussian amplitude distribution. The pulse probability is calculated conditional on EEG amplitude and time lag from an extended simultaneous recording of the pulse train of a single neuron and the EEG of the neighborhood in which the neuron is embedded. From Freeman 1975.

With a sufficiently large number of pulses the table of normalized conditional pulse probability reveals that single neurons are more likely to fire when the dendritic current of the population indicates excitation (Figure 6). About $\sim 10,000$ pulses are needed, which at typical rates for cortical neuronal background activity of ~ 3 p/s requires about an hour of continuous recording. Faster convergence occurs with multiple unit recording of the pulses in the local neighborhood around a microelectrode, provided the neurons belong to the same KI set. With respect to the mesoscopic order parameter, the individual neurons in a local neighborhood randomly rotate the burden of transmission by a form of time multiplexing. The mesoscopic pulse probability oscillations of the excitatory and inhibitory neurons have the same frequency in both the pulse and wave modes, but the phase of the inhibitory oscillations lags that of the excitatory oscillations by approximately a quarter cycle, as predicted by analysis of linearized negative feedback models (Freeman 1975). By the ergodic hypothesis the time ensemble average for a single neuron is inferred to correspond to the spatial ensemble average over the KI population in each single time frame.

The KII set corresponding to a single area of cortex has point and limit cycle attractors, which are revealed by steady state nearly flat or nearly periodic types of activity. However, these patterns are revealed only under abnormal conditions, such as deep anesthesia or surgical isolation. Normally each area interacts with others by negative and positive feedback through long axonal pathways with delays exceeding the relaxation times of dendritic integration (Figure 4, "open loop"), giving a KIII set (Freeman 1992). The characteristic frequencies of KII sets are incommensurate, and the feedback on piecewise linearization gives both negative and positive Lyapunov exponents. Since the KIII set contains multiple KI_e sets that provide excitatory bias, there is a global chaotic attractor that governs the generation of the continuous and robust aperiodic background activity.

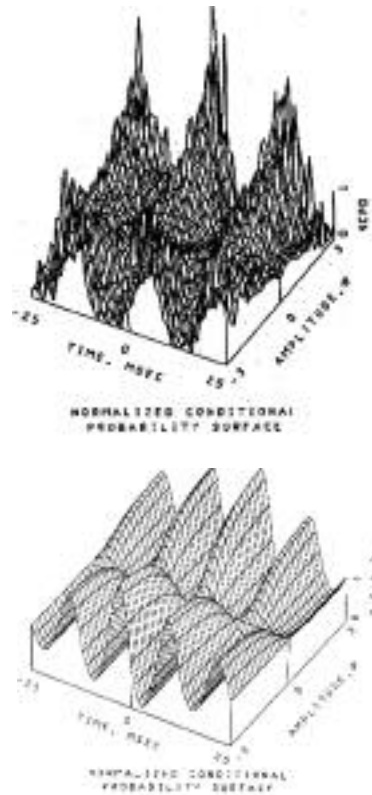


Figure 6. (a, upper frame) The normalized conditional pulse probability is shown for an excitatory neuron in the bulb in relation to the EEG generated by the bulbar inhibitory interneurons. The negative feedback accounts for the quarter cycle phase lead of the maximal pulse probability of the excitatory neuron preceding the maximal activity of the inhibitory interneurons in a negative feedback loop. (b) The lower frame shows a theoretical model fitted to similar data, from which the asymmetric sigmoid curve is derived. From Freeman 1975.

Whereas the stability of the KI_e set is firm, the stability of the KII set is conditional. The reason is found in the form of the pulse probability conditional on amplitude (Figure 6), which at the crests of the excitatory current in the extracellular tissue (the sum of the same currents that control neural firing probabilities) reveal an asymmetric sigmoid curve (Freeman 1992). The lower asymptote is determined by the distribution of thresholds for firing pulses. The upper asymptote is determined by the refractory periods. Between the rest level determined by the KI_e excitatory bias and the upper asymptote lies the point of maximal steepness of the slope, which specifies the nonlinear gain. This offset is due to the fact that the neurons in cortical populations spend 99% to 99.9% of their lifetimes below threshold in a near-linear state of readiness to fire, while their dendrites sum currents in a linear range of dendritic dynamics. In accordance with the ionic properties of the firing mechanism, as a neuron is excited by input, its probability of firing increases exponentially. That exponential increase in the population is revealed by the displacement of the maximal gain to the excitatory side of rest for the dendritic current. Excitation by sensory stimulation not only increases wave and pulse densities; it also increases the interaction strengths within the population, its feedback gains. Under appropriate conditions established in behavior by learning and by motivation (Freeman 1991), sensory input can destabilize a sensory area, so that it jumps out of its basal state into some other attractor in the landscape determined by learning.

4. Spatially coherent oscillations

This state transition carries the entire area into a new basin of attraction, which is selected by the sensory stimulus. Multichannel recording of EEGs in areas < 2 cm in diameter reveal a high degree of coherence; when measured by principal components analysis the dominant component contains well in excess of 80% of the total variance and not uncommonly $>95\%$. In the olfactory system the new basin is characterized by a spatial pattern of narrow band oscillations in the gamma range (Figure 7). These destabilizations

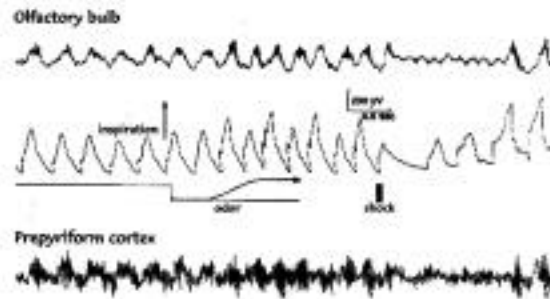


Figure 7. The traces show the bulbar EEG (top), prepyriform EEG (bottom) and the respiration in a single 6 s trial of a rabbit trained by classical aversive conditioning to respond to an odorant by sniffing. The slow wave is due to depolarization of the bulb by the pulses from the receptors on inspiration. The oscillatory gamma bursts result from destabilization by an increase in input-dependent gain by the asymmetric sigmoid function. From Freeman and Schneider 1982.

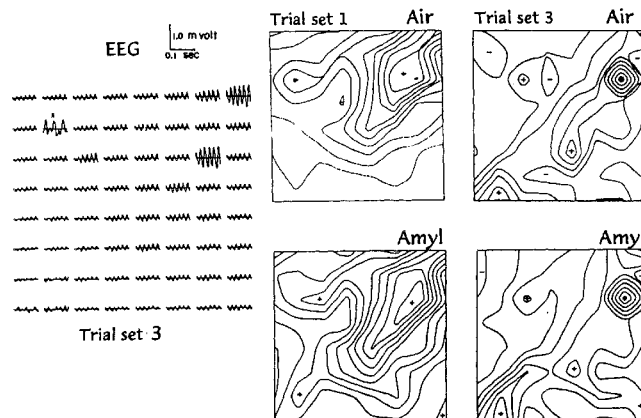


Figure 8. The left frame shows 64 EEG traces (bandpass filtered 20-80 Hz to give the gamma bursts) in an 8x8 array (4x4 mm) on the bulbar surface; one trace (x) sampled the prepyriform EEG. The right frames show contour plots of the AM patterns in the control state (Air) and under odorant stimulation (Amyl) after training to sniff. Trial set 3 shows the changes in patterns with the same stimuli after continued training, reflecting the dependence of the AM patterns on context and the value assigned by the unconditioned stimulus (in this case the shock). From Freeman and Schneider 1982.

occur repeatedly at the rate of respiration, giving a burst lasting 80 - 120 ms with each inhalation, which is superimposed on the peak of a wave of excitation driven by the receptor input. Each of these bursts occupies the entire olfactory bulb, which is the specialized cortical area that receives the axons of the olfactory receptors in the nose. Recording from multiple electrodes simultaneously (64 channels in an 8x8 array covering about 4x4 mm of the roughly 1 cm² surface of the olfactory bulb) shows that the shared wave form of gamma oscillation (Figure 8) in each burst has a reproducible spatial pattern, within trial sets and stimulus conditions, of amplitude modulation (AM). This AM pattern is transmitted by the bulb to other parts of the brain, particularly its main target, the olfactory (prepyriform) cortex, by the pulse trains of its projection neurons, which are constrained into pulse probability waves by the gamma burst, making it a carrier wave as well as an order parameter (Haken 1983).

It is important to note that these bursts of oscillation are mesoscopic, and that the microscopic neurons that generate the burst and are constrained by it in their firing probabilities do not directly reveal their participation. An example in Figure 9 compares the

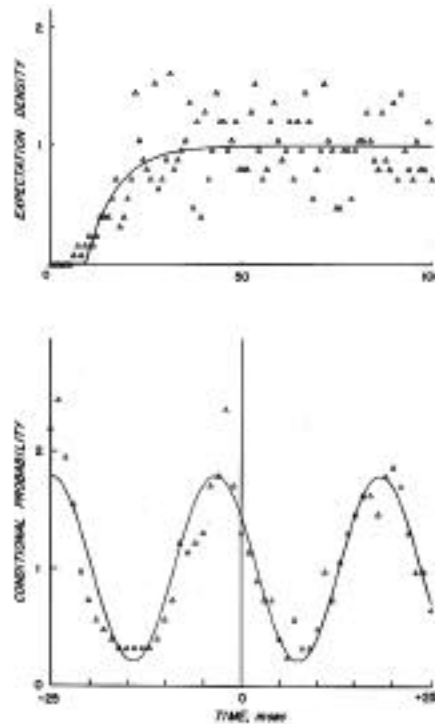


Figure 9. The autocorrelation (expectation density) of a single neuron computed from its pulse train reveals the refractory periods but no oscillation. The normalized conditional pulse probability from the same microscopic pulse train calculated using the EEG reveals prominent mesoscopic oscillation.

autocorrelation (expectation density) of a pulse train, which reveals the absolute and relative refractory periods but no oscillation. The probability of firing conditional on EEG amplitude for the same pulse train reveals an oscillation at the frequency of the EEG with a strong modulation amplitude. This disparity is because the burst frequencies in rabbits range typically from 40 to 90 Hz, whereas the pulses come at 1 - 10 p/s, so that each neuron fires on average at most only once every 4 cycles and usually much less often. The neurons are largely autonomous, firing occasionally as they need to in order to stay alive and healthy, because unlike transistors with a long shelf-life, inactive neurons tend to

atrophy and die. They are densely but sparsely interconnected with only 1% of the neurons having cell bodies within the radius of their dendritic and axonal arbors (Braitenberg and Schüz 1991). The small impact of each synapse gives only ~10 microvolts excitation toward a threshold of 1 or more millivolts (Amit 1989), so at least a hundred excitatory pulses in excess of inhibitory pulses must converge synchronously. For example, a cortical neuron may have 10,000 synapses, of which 85% are excitatory. At a modest mean rate of 1 p/s for pulses lasting 1 ms it receives about 10 p/s. A mean passive time constant for temporal integration of 10 ms allows depolarization to approach 1 millivolt. The fraction of the total variance that is covariant with the mesoscopic state of the population can be estimated as between 0.1% and 1% on the basis of their statistical properties (Freeman 1975; Abeles 1991; Kreiter, Aertsen and Gerstein 1989). That small fraction is crucial for brain function in carrying some neurons above threshold, particularly owing to the input-dependent gain of the population which is endowed by the asymmetric sigmoid nonlinearity of neural populations (Freeman 1992). Thus there is a stark contrast between the low-frequency chaos of the mesoscopic burst, and the essentially white noise of the collection of microscopic neurons comprising the population (Freeman 1999).

Another major difference between the microscopic neurons and the mesoscopic population is the spatial coherence of the gamma oscillations produced by cooperative interactions of the neurons. The correlations between pulse trains are usually insignificant (Abeles 1991), except under circumstances where selected neurons receiving afferent axons are driven by sensory stimuli, and the responses modulated by the gamma interactions are time-locked averaged with respect to stimulus onset (Singer and Gray 1995; Eckhorn 1991). But the synchrony of gamma oscillations is not at zero time lag, as it is found to be with time ensemble averaging across trials. Each AM pattern is accompanied by a spatial pattern of modulation of the phase of the 64 EEG traces at the shared instantaneous frequency. The phase values are most easily calculated at the center frequency of each burst by using nonlinear regression to fit the sum of two cosine basis functions that are linearly modulated in frequency and amplitude over time (Freeman 1992). The phase of the spatial ensemble average with respect to the time window of observation serves as the phase reference inside the window. After optimal spatial and temporal filtering of the 64 EEG traces from single bursts, the 64 values of phase reveal orderly spatial patterns.



Figure 10. The upper frame shows the AM pattern of a burst from the prepyriform cortex. The input path runs left to right under the flanking peaks of amplitude. The lower frame shows the phase pattern, with a shallow gradient along the path where the conduction velocity is highest, and steep gradients toward the edges where the smaller branches are more slowly conducting. The phase pattern can be fitted with a cone, for which the maximal lead is always at the anterior end upon bulbar driving. From Freeman 1978.

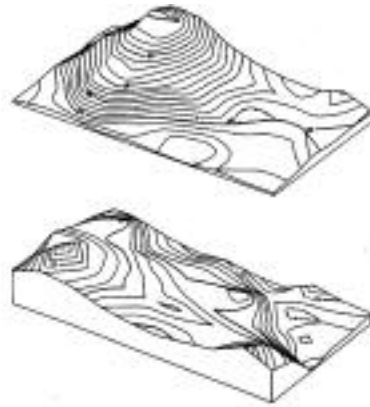


Figure 11. The upper frame shows the bulbar AM pattern. The location of the peak depends on prior training. The lower frame shows the EEG phase pattern. The direction of the slope varies randomly and seldom conforms to that of the input path (right to left), and a maximum (lead) or minimum (lag) occasionally occurs within the array, which suggests that a cone is a proper form to fit the data. From Freeman 1978.

Examples are contrasted of the amplitude and phase patterns of single EEG bursts observed with a 6x10 array of 60 electrodes (4x7 mm window) on the prepyriform cortex (Figure 10) and the olfactory bulb (Figure 11). Both of these forebrain areas contain populations of interacting excitatory and inhibitory neurons. Both have input pathways that run across the windows of observation, from left to right in Figure 10 and from right to left in Figure 11. Both have impulse responses on electrical stimulation of their input axons that can be fitted with damped cosines. And the phase gradients of the damped cosines correspond in direction and steepness to the directions and conduction velocities of the afferent axons. This is seen most clearly in Figure 10, where the maxima of amplitude lie to either side of the main axis of the input pathway (upper frame) leaving a sort of valley through which the pathway runs, and the phase gradient is shallow from left to right over the main trajectory of the pathway (lower frame) where the velocity is highest, with steeper slopes on the edges, where the axons branch, diverge, and spread out like an alluvial fan with slow velocities. These patterns hold for both the evoked potential (the impulse response) and the EEG (the bursts driven by the output of the bulb, as indicated by the EEGs in Figure 7).

The duration of the spatially AM patterned bursts ranges from 80 - 120 ms with a mode near 100 ms. They appear to be separated by gaps of similar duration, corresponding to the respiratory rhythm in the bulb and prepyriform of 3-7 Hz in rabbits, and to the theta range in the neocortices, but there without relation to respiration. In the olfactory system the bursts result from the barrage of excitatory input from receptors to the bulb, leading to the hypothesis that the bulb is destabilized by each inhalation, owing to the asymmetric sigmoid undergoes a state transition from the control state to the burst state, and then transits back during exhalation (Freeman 1975; 1992), thus explaining the "induced" wave of gamma activity first described by Adrian (1950). The transition can be viewed as equivalent to a phase transition between gaseous and liquid states in a physical system.

The bulb and prepyriform differ in the following respects. First, the input path to the bulb is topographically organized, so that there is a rough mapping from the layer of olfactory receptor neurons in the nose onto the bulb, whereas the path from the bulb to the prepyriform is divergent-convergent (Figure 12). Each bulbar neuron has axonal branches

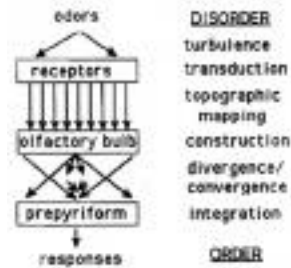


Figure 12. The input path from the receptors to the bulb is topographically organized, as are all projections from sensory receptors to primary receiving areas. The output path of the bulb to the prepyriform is divergent-convergent without topographic mapping. This kind of path effects a spatial integration of the signal transmitted, serving to enhance bulbar activity having a common instantaneous frequency and to attenuate any activity having phase and frequency dispersion. From Freeman 1990.

that spread broadly over the cortex, and each cortical neuron receives axons from neurons scattered widely over the bulb. This anatomical property provides a mechanism whereby the mesoscopic order parameter that is observed in the AM pattern is extracted as signal from the microscopic noise. The integration selects for the transmitted activity that has the same instantaneous frequency over the transmitting array of neurons, and it smoothes the activity that has frequency and phase dispersion, thus serving as a 'brain laundry' (Freeman 1991).

Second, the phase patterns of the responses of the prepyriform cortex to electrical stimulation and to bulbar driving are the same, but this correspondence does not hold for the bulb. As in the cortex the oscillatory bulbar electrically evoked impulse response has a linear phase gradient that corresponds to the direction (right to left in Figure 11) and velocity of the input axons running over the bulbar surface (Freeman 1975). In contrast, the bulbar EEG gamma burst induced by inhalation has a phase gradient that often appears at first glance to be linear though noisy (as shown in Figure 11), but which changes in direction at random from each burst to the next, without regard either to the conditioned stimulus or to the direction of the input pathway.

Third, the AM patterns of prepyriform impulse responses appear to be independent of which part of the bulb is stimulated, but the AM pattern of the bulbar impulse responses depends on which part of the input path to the bulb is stimulated by a focal electrical stimulus. The odorant-induced gamma bursts in the bulb have AM patterns that depend on prior learning by behavioral conditioning, and they do not conform to electrically evoked patterns, but the majority (>80%) of prepyriform bursts have phase gradients that match the trajectory of its input path from the bulb (Freeman et al. 1995), and the remainder have phase gradients indicating that the prepyriform can also be driven intermittently from sites in the limbic system, particularly the entorhinal cortex (Freeman 1973; Kay and Freeman 1998).

5. Radial phase gradients and their origin and significance

The 64 values of phase can be fitted by nonlinear regression with either a plane or a cone in spherical coordinates for the bulb (Freeman and Baird 1987) and in planar coordinates for the prepyriform cortex and the neocortices (Freeman et al. 1995). The fitted cone consistently gives lower residuals. The phase cone in each bulbar burst (Figure 13) is like

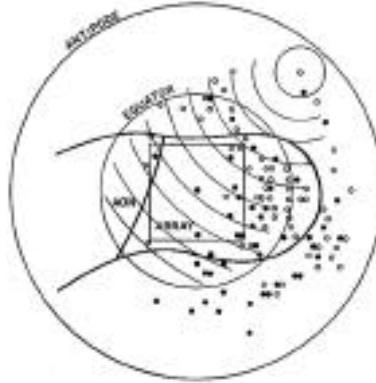


Figure 13. The rabbit bulb is shown in outline, with the array indicated by the rectangle. The bulbar surface has the form of a punctured sphere; it has been flattened for display of the apices. The sign of the apices varies randomly between lead (solid dots) and lag (open dots), and the location may be anywhere except in the posterior quadrant where axons leave and enter the bulb. The circular isophase contours are in steps of 0.1 radian. From Freeman and Baird 1987.

the pattern of wave spread when a stone is dropped into still water (Freeman and Baird 1987). The velocity of the wave front is sufficiently high that the total delay across the bulb in the rabbit is under a quarter of the cycle duration at the modal peak frequency (70 Hz). The location of the apex on the bulb surface and its sign (maximal phase lead or lag) vary randomly without relation to odor stimuli, and the gradients have no spatial relation to sensory or centrifugal axonal pathways. The array covers only 20% of the bulb surface in the rabbit, so that most apices are sited by extrapolation outside the array. The mean interelectrode phase differences is about 2° with an average maximal difference across the array of $<10^\circ$. Spatial filtering of the real and imaginary parts of the spectra improves phase resolution, so then on average the cone incorporates $>65\%$ of the variance of the phase data. The conic surface also serves to fit the prepyriform gamma bursts, but the apex is invariably a minimum (phase lead) with a fixed location at the anterior or posterior edge of the array (Figure 10), reflecting bulbar or limbic driving.

I propose the hypothesis that the bulbar phase cone is a residue of the state transition by which each burst forms. In spatially dispersed media such transitions do not occur everywhere simultaneously. They start at a site of nucleation and spread in all directions, as in the formation of a raindrop or a snowflake. The locations of the apices show that when sensory input destabilizes the bulb, the burst transition may begin anywhere in the bulb (except in the posterior quadrant where axons maintain connections with the brain), and from that locus it is spread by axon collaterals of neurons in the bulb. Mean phase velocity is 1.80 ± 0.43 in m/s, the estimated conduction velocity of bulbar axon collaterals. The phase pattern is preserved through the burst, apparently because the intracortical connectivity is too sparse and the autonomy of the neurons is too great to support entrainment and phase locking. Measurements of the phase gradient and center frequency of bulbar bursts indicate that the cumulative phase dispersion with distance over the entire bulb does not exceed $\pm 45^\circ$, which is the half power point under spatial integration of the burst, as it forms by global cooperation. Interaction strength may not weaken with distance owing to the fact that propagating pulses do not attenuate with distance, but it must weaken if the oscillations go out of phase with distance. The half power point also sets a convenient limit to the effectiveness of the spatial integration performed by prepyriform neurons receiving convergent axons from the bulbar divergent output pathway, the brain

laundry, because further phase dispersion would result in increasing degradation of the bulbar output.

Axon collaterals of bulbar neurons rarely extend more than a mm or about 10% of the distance around the bulb, but some deep axons of tufted cells cross through its core and can account for the global coherence of the bulbar EEG. The transition velocity is a group property that differs distinctly from the slow process of polysynaptic transmission with cumulative synaptic delays, which would require in excess of 100 ms to pass over the entire bulb (Freeman 1975), suggesting that the transition manifests "anomalous dispersion" (Freeman 1990). An example from physics is the sound from a blow with a hammer at one end of a metal bar that reaches the other end long before the energy of the mechanical impulse does. It appears that when the bulb is brought by receptor input to the threshold for a chaotic state transition, it becomes exquisitely sensitive, enabling those few axons that travel long distances to precipitate and extend the state transition from the site of nucleation where it begins.

6. Boundary conditions in the neocortex

Analysis of phase patterns has also been done on EEGs from the visual, auditory and somatosensory neocortices (Barrie, Freeman and Lenhart 1996). The analysis is more difficult because the neocortices lack the relatively narrow spectral peaks in the gamma range that characterize the olfactory EEGs, so the measurement of phase is less precise, and they lack the equivalent of respiratory waves, which facilitate EEG segmentation for the identification of olfactory gamma bursts. Neocortical phase cones are tracked with a time window lasting 64 ms that is stepped in 2 ms intervals along the set of 64 traces. In each window a cone is fitted to the phase values from the dominant cosine fitted to the 64 EEGs. A cone is detected when the residual of the cone fit falls below 30%, and it ends when the residual rises to 50% in later steps, provided that the sign and location of the apex do not change.

Representative values of the cones are shown in Figure 14. Mean residuals of fitted cones

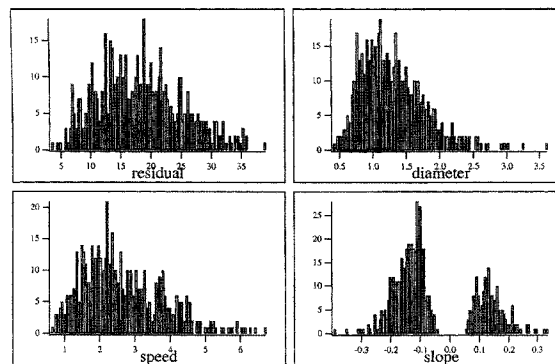


Figure 14. The distributions are shown of the average % residuals from fitting a cone to the 64 neocortical EEG traces after temporal filtering (20-80 Hz) to extract the gamma activity and spatial filtering (low pass at 0.29 c/mm) to enhance phase measurement. The diameters are in cm; the phase velocity is in m/s; the slopes are in radians/mm.

range between 5% and 35%. The modal diameter is 1.2 cm with a range from 0.5 to 2.5 cm. The modal velocity is 2.2 m/s, and the modal value of the slope in radians/mm is ± 0.12 ($\pm 7^\circ/\text{mm}$). The values for slope and diameter are independent of the center

frequency, which ranges from 30 to 70 Hz. The durations of the cone segments are skewed, with no clear cut-off for short durations, a tail extending to 140 ms, and a median value of 86 ms. The distribution of intervals between cones is also skewed, with a median value near 300 ms and a mean near 100 ms. The histogram of the incidence of cones in a representative session of 40 trials is shown in Figure 15, lower frame, from the stimulus

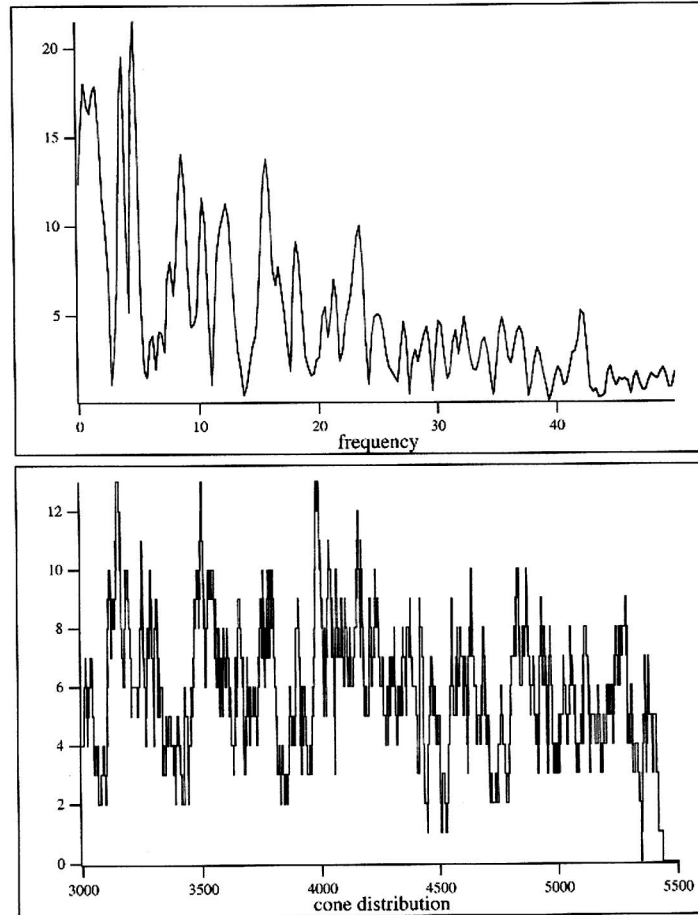


Figure 15. The results are summarized from 40 trials in one training session of a rabbit trained to respond to a visual cue (Barrie et al. 1996). The time base in ms begins with the arrival of the conditioned stimulus (a bright flash discriminated from a dim flash). The cones tend to recur at peak frequencies in the theta range (3-7 Hz), and the peaks in the cone distribution indicate that the flash tends to re-set the recurrence of the cones.

arrival at 3000 ms to the completion of conditioned responses by 5600 ms. The upper frame is the Fourier transform of the histogram to show the peak repetition rates in the theta range, comparable to those in the olfactory system but by different neural mechanisms. Whether neocortical state transitions are self-organizing or require putative sources of activation to drive them as in olfaction is unknown.

The phase cones offer a solution to a puzzling problem concerning the boundary conditions of neocortical activity. Simultaneous recordings from different parts of the neocortex, such as the primary sensory areas and parts of the limbic system as schematized for the rabbit in Figure 16, show differing time series. An example is shown in Figure 17 of the EEGs that



Figure 16. The locations of the recording sites on the rabbit left hemisphere are indicated by the rectangles (bulb, OB; prepyriform, PPC; somatosensory, SOM; auditory, AUD; visual, VIS; and entorhinal (limbic) ENT). Adapted from Barrie et al. 1996.

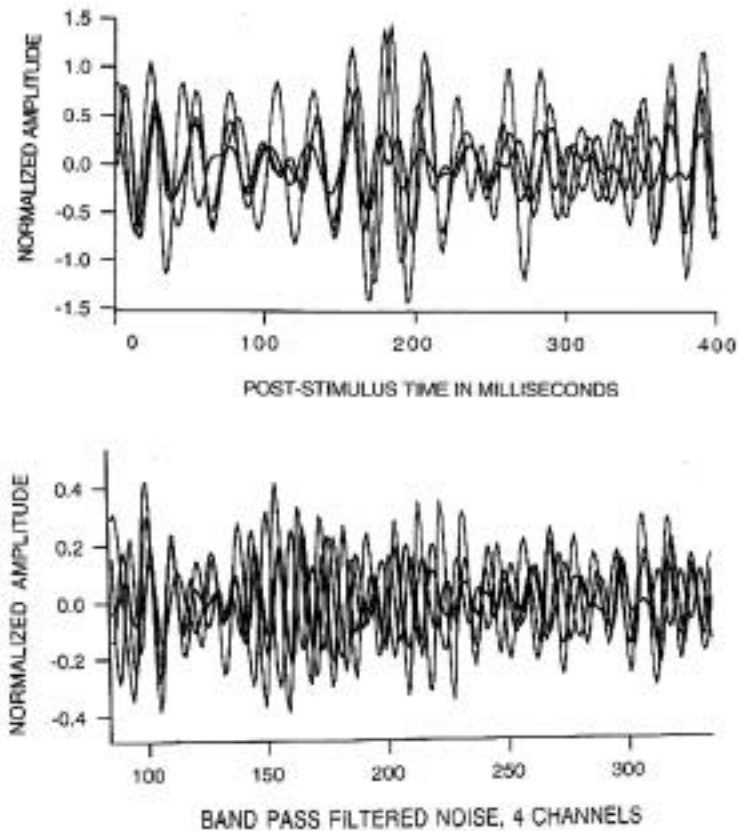


Figure 17. Upper frame: EEGs from the several areas are superimposed after they are filtered in the gamma range, showing the similarity of wave forms but the diversity of phase relations. There is no evidence of phase locking at times expected from the temporal locations of the stimuli, responses, or AM patterns. Lower frame: white noise is simulated with random numbers (normally distributed with zero mean and unit standard deviation) independently on four traces filtered in the same manner as the EEGs. Both sets show a tendency to intermittent phase locking at unpredictable times, which has also been observed in EEG recordings from the cortical surface of humans undergoing brain surgery (Menon et al. 1996).

were recorded from the four primary sensory areas and the entorhinal cortex and superimposed after filtering to display the gamma range. There is little direct evidence of phase locking between these sites, and the shared variance by principal components

analysis is no more than 50%, in contrast with multiple traces from local areas. The differences imply that some sort of boundary must separate the local regions that are responsible for spatially coherent oscillations. The neocortex has no anatomical boundaries corresponding to those that demarcate the olfactory bulb, prepyriform, and other parts of the paleocortex. Each cerebral hemisphere consists of a continuous sheet of interconnected neurons, though local differences in cytoarchitecture abound, and a variety of structures exists in the submillimeter spatial scale, well below the mm to cm range of AM patterns. Essentially the neocortex of each hemisphere is a unified organ of the brain, and yet it has the capacity for dynamic segregation into functional subunits of varying size and location. It appears that the delay in self-organizing processes imposed by axonal conduction times, which is expressed in the radial phase gradients, may provide the necessary functional boundary conditions.

Still, the requirement exists for functional cooperation among AM patterns, so that some degree of synchronization must exist between different sites, in order for brains to organize effective behavior. The physiological evidence for this coordination remains elusive, as seen by comparing the EEG recordings (Figure 17, upper frame) with the same number of traces of independent white noise (random numbers with zero mean and unit standard deviation) that were band-pass filtered in the same way as the EEGs (lower frame) to enhance the gamma activity (colored noise). There are subtle differences in appearance between the two sets that suggest a higher degree of order in the EEG, but they are still beyond firm grasp.

7. Discussion

The results support the hypothesis that each sensory neocortex as well as the bulb is governed by an attractor landscape with multiple basins (Freeman 1995). Each basin is formed by Hebbian learning under conditioning to respond with discrimination to a particular class of stimuli. The variations within each class serve to define the basin of attraction, and the spatial AM pattern of the carrier wave defines the attractor and the cortical output. The existence of phase cones in neocortical EEGs indicates that axonal transmission is the basis for the establishment of mesoscopic cooperative neocortical domains, and that axonal delays impose limitations of the size of such domains in two respects: the establishment of cooperation, and the readout under spatial divergence in the transmitting pathway, both of which are degraded by phase dispersion. The lack of radial phase gradients in the prepyriform EEGs indicates that, whereas the sensory cortices and the bulb construct AM patterns under the impact of sensory stimuli, the prepyriform does not, but instead operates on the oscillations that are imposed on it by the bulb and by the limbic system (Kay and Freeman 1998), which are characterized by unequivocal phase lags owing to the propagated action potentials that carry the bulbar signals. The prepyriform cortex does not create mesoscopic spatial patterns deriving from its own endogenous state transitions but is driven by bulbar and limbic transmissions.

In keeping with this inference, the bulbar and prepyriform EEGs are highly correlated with each other during bursts (Bressler 1988), though between bursts and in the basal rest state the time-lagged correlations indicate that the shared covariance is less than 10% of the total variance. No other pairs of sensory cortices give EEGs that are so strongly and continually correlated, though intermittent high levels of correlation have been reported between widely separated areas of cortex during learned behavior (Bressler et al. 1993). The question arises whether the outputs of the primary sensory areas for vision, hearing and touch drive other cortical or subcortical masses as satellites, in the manner that the bulb drives the prepyriform cortex and receives its output by distributed feedback, and, if so, where these putative satellites are located, and how they operate as controllers of the chaotic dynamics of pattern recognition in the primary areas. The satellites are not likely to be revealed by

linear correlation or coherence techniques and may be resistant to analysis by existing nonlinear methods as well.

The delay imposed by axonal transmission brings into question reports of "zero phase lag" between cortical sites separated by several mm or even located in different hemispheres (Engel et al. 1991). One explanation is that the reports are based on temporal ensemble averages over data in which the high variance among individual measurements reflect delays in both directions. When phase differences between bulbar sites are averaged over trials, the only possible outcome is an average of zero. Another cause is inadequate specification of confidence intervals. Menon et al. (1996) have shown that EEGs from multiple sites on human cortex from 8x8 arrays with 1 cm spacing give intermittent segments lasting 50 - 100 msec of high positive and negative correlation coefficients, and so also do time series of random numbers that are spaced at the digitizing interval of the EEGs, and filtered at the same band width (20 - 50 Hz), although, consistent with the findings in animals, there is a striking excess of positive correlations between traces taken from pairs of electrodes < 2 cm apart.

Several investigators have attempted with models of microscopic interactions to explain the challenging finding of 'zero lag' correlation between the gamma oscillations of neurons separated by millimeter distances (Roelfsema et al. 1997). Nunez (1981) models large scale coupled oscillations in brains as standing waves based on hemisphere-wide boundary conditions. Engel et al. (1991) models zero delay correlations between remote sites with two coupled oscillators, each entraining the other. Usher, Schuster and Niebur (1993) and Schillen and König (1994) model the phenomenon by assuming that the feedback delay within a target matches the transmission delay between the transmitter and its target in an excitatory feedback network. Traub et al. (1996) overcome some of the rigidity of that model by invoking doublet firing of single neurons, which they show is enhanced in states of high amplitude gamma. The tendency of neurons embedded in excitatory feedback networks to fire twice on impulse input is well known (Freeman 1975), and the increase in gain of the excitatory positive feedback loop with learning has been shown to increase gamma amplitude substantially (Freeman 1992), so these models are consistent with the interpretation that gamma oscillations are mesoscopic, although they do not explain the average quarter-cycle phase lag of the inhibitory neural firing with respect to the excitatory firing, which is essential for mesoscopic explanation (Freeman 1975, 1992), nor do they explain observed local phase gradients in phase cones, nor the marked tendencies of most cortical neurons to fire aperiodically.

8. Summary

Neural activity in the cerebral cortex has at least three levels of organization. Microscopic activity is observed in the pulse trains of axons of individual neurons. Macroscopic activity is observed in whole brains by imaging techniques such as fMRI and PET. Between these at the mesoscopic level (Freeman 2000) brain activity is observed in the AM and phase patterns of electrical fields of potential that are established by neuron populations through the flow of summed dendritic current across the extracellular resistance of cortical tissue. The EEG oscillations are typically aperiodic with broad spectra decreasing approximately "1/f²" in log power with log frequency, often with excess power in well-known ranges. The wave forms are spatially coherent over domains on the order of 1 to 2 cm in diameter, which implies that the single neurons that create the dendritic fields have a degree of synchronization in their firing of pulses. The shared wave forms in sensory cortices display brief epochs lasting ~ 100 ms, which have spatial patterns of amplitude modulation (AM) that are related to behavior and reflect perception of sensory stimuli that is established through learning. However, the oscillations in primary sensory areas at the mean

frequency are not precisely in synchrony, owing to axonal propagation delays. The spatial pattern of phase of the AM patterns is radially symmetric in the form of a cone, for which the gradient in m/s is consistent with the conduction velocities of the axons running parallel to the cortical surface. The sign at the conic apex is either maximally negative (lead) or positive (lag), and it varies randomly in successive epochs without relation to perceptual content. The hypothesis is proposed that the shared activity revealed in the dendritic potentials is due to a small fraction of the total variance of the largely autonomous neurons, whose interactions constrain the neurons to give a low but significant level of covariance, and that the activity is transmitted not by topographic mapping but by divergent-convergent pathways that extract the covariant signal by spatial integration. The location of the apex of the phase cone manifests the site of nucleation of state transitions by which each AM pattern is formed by symmetry breaking, and the obligatory phase lag in the establishment of the pattern defines the boundary condition of each AM pattern, both in respect to formation by cortical neuronal interaction and to read-out under dendritic integration by the target neurons of cortical transmissions. The level of effective synchronization is not absolute but is to be assessed in terms of the effectiveness of the neural mechanism by which cooperative signals are extracted from noise. A similar low degree of covariance may serve to coordinate mesoscopic domains into macroscopic ordered brain states.

References

- Abeles M (1991) *Corticonics: Neural Circuits of the Cerebral Cortex*. Cambridge UK: Cambridge University Press.
- Adrian ED (1950) The electrical activity of the mammalian olfactory bulb. *Electroencephalography and clinical Neurophysiology* 2: 377-388.
- Amit DJ (1989) *Modeling brain function: The World of Attractor Neural Networks*. Cambridge UK: Cambridge University Press.
- Bollabás B (1985) *Random Graphs*. New York NY: Academic Press.
- Braitenberg V, Schüz A (1991) *Anatomy of the Cortex: Statistics and Geometry*. Berlin: Springer-Verlag.
- Bressler SL (1988) Changes in electrical activity of rabbit olfactory bulb and cortex to conditioned odor stimulation. *Journal of Neurophysiology* 62: 740-747.
- Bressler SL, Coppola R, Nakamura R (1993) Episodic multiregional cortical coherence at multiple frequencies during visual task performance. *Nature* 366: 153-156.
- Eckhorn R (1991) Principles of global visual processing of local features can be investigated with parallel single-cell- and group-recordings from the visual cortex. In Aertsen A, Braitenberg V (Eds.), *Information Processing in the Cortex* (pp. 385-420). Berlin: Springer-Verlag.
- Engel AK, Kreiter AK, König P, Singer W (1991) Synchronization of oscillatory neuronal responses between striate and extrastriate visual cortical areas of the cat. *Proceedings, National Academy Sciences USA* 88: 6048-6052.
- Freeman WJ (1973) Cinematic display of spatial structure of EEG and averaged evoked potentials (AEPs) of olfactory bulb and cortex. (Abstract) *Electroencephalography and clinical Neurophysiology* 37: 199.
- Freeman WJ (1975) *Mass Action in the Nervous System*. New York NY: Academic Press.
- Freeman WJ (1978) Spatial properties of an EEG event in the olfactory bulb and cortex. *Electroencephalography and clinical Neurophysiology* 44: 586-605.
- Freeman WJ (1990) On the problem of anomalous dispersion in chaoto-chaotic phase transitions of neural masses, and its significance for the management of perceptual information in brains. In: Haken H, Stadler M (eds.) *Synergetics of Cognition*. Berlin: Springer-Verlag. Volume 45: 126-143.
- Freeman WJ (1991) The physiology of perception. *Scientific American* 264: 78-87.
- Freeman WJ (1992) Tutorial in Neurobiology: From Single Neurons to Brain Chaos. *International Journal of Bifurcation and Chaos* 2: 451-482.

- Freeman WJ (1995) *Societies of Brains*. Mahwah NJ: Lawrence Erlbaum Associates.
- Freeman WJ (1999) *How Brains Make Up Their Minds*. London UK: Weidenfeld and Nicolson.
- Freeman WJ (2000) *Mesoscopic Brain Dynamics*. London UK: Springer-Verlag. (Feb.)
- Freeman WJ, Barrie JM (2000) Analysis of spatial patterns of phase in neocortical gamma EEGs in rabbit. *Journal of Neurophysiology* 84: 1266-1278.
- Freeman WJ, Barrie JM, Lenhart M, Tang RX (1995) Spatial phase gradients in neocortical EEGs give modal diameter of "binding" domains in perception. Abstracts, *Society for Neuroscience* 21: 1649 (648.13).
- Freeman WJ, Baird B (1987) Relation of olfactory EEG to behavior: Spatial analysis: *Behavioral Neuroscience* 101: 393-408.
- Freeman WJ, Jakubith S (1993) Bifurcation analysis of continuous time dynamics of oscillatory neural networks. In: Aertsen A, von Seelen W (eds.) *Brain Theory - Spatio-temporal Aspects of Brain Function*. Amsterdam, Elsevier. pp. 183-208.
- Freeman WJ, Schneider W (1982) Changes in spatial patterns of rabbit olfactory EEG with conditioning to odors. *Psychophysiology* 19: 44-56.
- Haken H (1983) *Synergetics: An Introduction*. Berlin: Springer-Verlag.
- Kay LM, Freeman WJ (1998) Bidirectional processing in the olfactory-limbic axis during olfactory behavior. *Behavioral Neuroscience* 112: 541-553.
- Kreiter AK, Aertsen AMHJ, Gerstein GL (1989) A low-cost single-board solution for real-time unsupervised waveform classification of multineuron recordings. *Journal of Neuroscience Methods* 30: 59-69.
- Menon V, Freeman WJ, Cutillo BA, Desmond JE, Ward MF, Bressler SL, Laxer KD, Barbaro NM, Gevins AS (1996) Spatio-temporal correlations in human gamma band electrocorticograms. *Electroencephalography and clinical Neurophysiology* 98: 89-102.
- Nunez PL (1981) *Electric Fields of the Brain: The Neurophysics of EEG*. New York NY: Oxford University Press.
- Ramón y Cajal S (1911) *Histologie du Systeme Nerveux de l'Homme et des Vertèbres* (Vols. I & II). Paris: Maloine.
- Rapp P (1993) Chaos in the neurosciences: Cautionary tales from the frontier. *Biologist* 40: 89-94.
- Robinson PA, Rennie CJ, Wright JJ, Bourke PD (1998) Steady states and global dynamics of electrical activity in the cerebral cortex. *Physical Review E* 58: 3557-3571.
- Schillen TB, König P (1994) Binding by temporal structure in multiple feature domains on an oscillatory neuronal network. *Biological Cybernetics* 70: 397-405.
- Singer W, Gray CM (1995) Visual feature integration and the temporal correlation hypothesis. *Annual Review of Neuroscience* 18: 555-586.
- Traub RD, Whittington MA, Stanford IM, Jefferys JGR (1996) A mechanism for generation of long-range synchronous fast oscillations in the cortex. *Nature* 383: 421-424.
- Usher M, Schuster H-G, Niebur E (1993) Dynamics of populations of integrate-and-fire neurons, partial synchronization and memory. *Neural Computation* 5: 570-586.